

GABFusion: Rethinking Feature Fusion for Low-Bit Quantization of Multi-Task Networks

Zhaoyang Wang¹, Dong Wang¹

¹Institute of Information Science, Beijing Jiaotong University
No.3 Shangyuan Village, Xizhimenwai, Haidian District, Beijing, China, 100044

Abstract

Despite the effectiveness of quantization-aware training (QAT) in compressing deep neural networks, its performance on multi-task architectures often degrades significantly due to task-specific feature discrepancies and gradient conflicts. To address these challenges, we propose Gradient-Aware Balanced Feature Fusion (GABFusion), which dynamically balances gradient magnitudes and fuses task-specific features in a quantization-friendly manner. We further introduce Attention Distribution Alignment (ADA), a feature-level distillation strategy tailored for quantized models. Our method demonstrates strong generalization across network architectures and QAT algorithms, with theoretical guarantees on gradient bias reduction. Extensive experiments demonstrate that our strategy consistently enhances a variety of QAT methods across different network architectures and bit-widths. On PASCAL VOC and COCO datasets, the proposed approach achieves average mAP improvements of approximately 3.3% and 1.6%, respectively. When applied to YOLOv5 under 4-bit quantization, our method narrows the accuracy gap with the full-precision model to only 1.7% on VOC, showcasing its effectiveness in preserving performance under low-bit constraints. Notably, the proposed framework is modular, easy to integrate, and compatible with any existing QAT technique—enhancing the performance of quantized models without requiring modifications to the original network architecture.

Introduction

In recent years, quantization has become a pivotal technique for neural network model compression (Rokh, Azarpeyvand, and Khanteymooori 2023). By transforming the representation of network weights and activations from high-precision floating-point formats to low-bitwidth integer equivalents, quantization effectively minimizes both memory overhead and computational latency in deployment.

The majority of existing research on neural network quantization has concentrated on image classification tasks and can be broadly categorized into two paradigms: Post-Training Quantization (PTQ) and Quantization-Aware Training (QAT). PTQ compresses models efficiently via a single calibration pass and performs well at 8-bit precision. In contrast, QAT incorporates quantization into the training process and achieves significantly better accuracy retention at ultra-low bit-widths (≤ 4 bits), albeit at the cost of in-

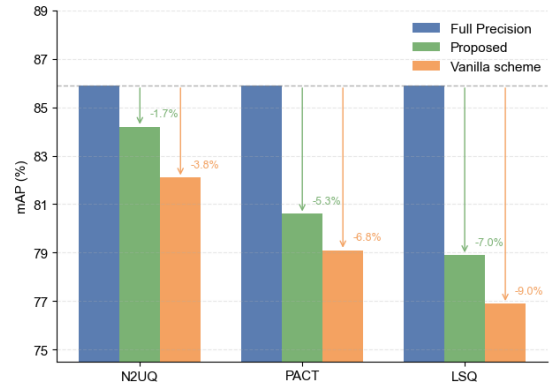


Figure 1: Comparison of the accuracy drop of the YOLOv5 model under 4-bit quantization across three representative QAT schemes, alongside the proposed approach. To ensure reproducibility, we include our reimplementations of the baseline methods in the **Appendix**.

creased training complexity. For instance, the recent work of N2UQ (Liu et al. 2022) even demonstrates accuracy improvements over its full-precision counterpart under 4-bit configurations.

However, the exploration of low-bitwidth quantization in the context of multi-task learning—particularly for architectures such as object detectors that perform both classification and regression tasks concurrently—remains relatively underdeveloped. A representative example is the YOLO family (Varghese and M. 2024; Wang et al. 2024) of object detectors, which are extensively deployed in both academic research and industrial applications. Current schemes are only capable of preserving near full-precision accuracy with 8-bit precision quantization, but suffers from substantial performance drops with low bit-width (Wang et al. 2023). As illustrated in Fig. 1, we apply three representative QAT approaches, including PACT, LSQ, and N2UQ, to quantize the widely adopted YOLOv5 model under a 4-bit precision. Even with N2UQ, the resulting quantized YOLOv5 model still exhibits a significant performance degradation of 3.8%.

The results of the above experiment suggest the existence of task-dependent quantization errors that are overlooked by

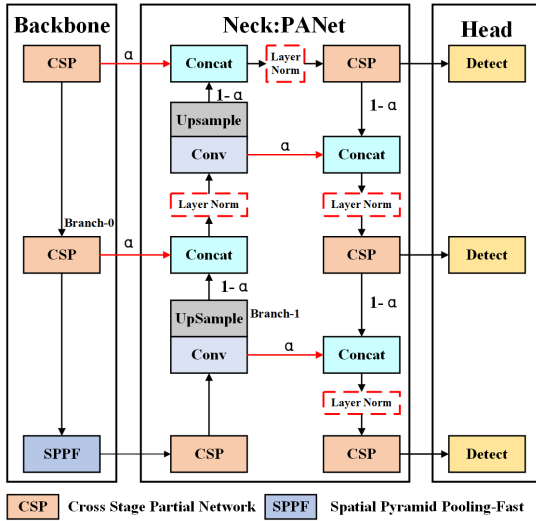


Figure 2: Architecture of the YOLOv5 object detection model.

current quantization approaches, leading to irreversible accuracy degradation during the quantization process. To reveal the underlying mechanism behind this issue, we first need to review the characteristics of the YOLO network. In what follows, we take YOLOv5 as a representative example, as subsequent variants follow similar architectural principles and detection paradigms. As illustrated in Fig. 2, YOLOv5 extracts features through a CSP backbone, fuses them via the PANet neck, and performs multi-task prediction using a detection head. In contrast to conventional classification networks that rely solely on the final semantic layer, YOLOv5 employs feature fusion (Liu et al. 2018) to coordinate the requirements of different tasks—an essential design for multi-task learning. This is because shallow layers are more adept at capturing fine-grained spatial details, making them suitable for regression tasks (He et al. 2017), while deeper layers encode global context and high-level semantics (Tong and Wu 2024), which are more suitable for classification tasks.

During the QAT process, each quantized layer introduces discretization noise, i.e., quantization error, which accumulates as the network deepens, causing a cascading effect (Colbert, Pappalardo, and Petri-Koenig 2023) and severe gradient oscillations (Ma et al. 2024) during training. Our study further reveals that, in multi-task architectures such as YOLO, it can be expected that quantization introduces significant gradient imbalance at each feature fusion point, i.e., the Concat layer: the shallow branches suffer from insufficient simulated noise, leading to restricted gradient flow, while the deep branches are disturbed by large accumulated quantization noise, hindering the optimization process.

To verify the correctness of our analysis, we further conducted an experiment to measure the gradient changes of the features responsible for different tasks during quantized training. We train YOLOv5 on the VOC dataset and track the average feature gradients of different branches at the first Concat layer in the neck, where shallow and deeper features

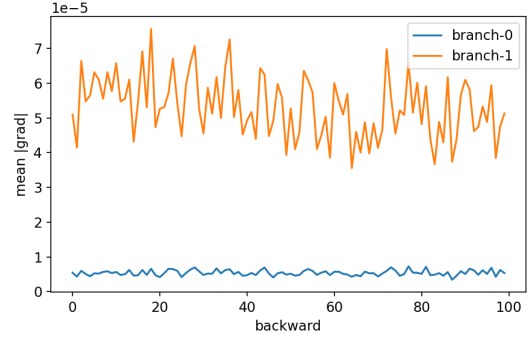


Figure 3: Measured average gradient magnitude at the feature fusion node in YOLOv5 during quantization.

are fused (as shown in Fig. 2). According to GradCAM (Selvaraju et al. 2017), larger gradients generally indicate that the model optimizes more actively towards the corresponding features. As shown in Fig. 3, branch-0 contains more fine-grained local features from shallow layers, which are crucial for bounding box regression. In contrast, branch-1 captures more high-level semantic features from deeper layers, which is important for classification. We observe that the network tends to focus on optimizing the deep semantic branch (branch-1) while neglecting the shallow local branch (branch-0), leading to biased gradient updates across tasks.

To tackle the aforementioned issue, we propose GABFusion (Gradient-Aware Balanced Feature Fusion), which is quantizer-agnostic and broadly applicable to various QAT algorithms. Firstly, GABFusion incorporates learnable dynamic scaling factors within different network branches before feature fusion. Subsequently, a layer normalization is inserted immediately after the feature fusion layer, serving as a plug-in component that performs gradient re-centering and re-scaling. This two-step approach enables GABFusion to effectively readjust the gradient distribution, mitigate biased gradient updates, and consequently improve the performance across all tasks of the quantized model.

From another perspective, the observed optimization bias arises from the incompatibility of conventional loss designs with quantized multi-task networks. These losses use the perturbations caused by quantized parameters and their deviations from the ground-truth values as supervision, aiming to reduce numeric discrepancies. However, due to the inherent nonlinearity and redundancy of neural networks, such low-level differences have limited influence on task performance, as predictions are driven by learned features rather than numerical deviations. To address this limitation, we propose a novel feature-level loss supervision strategy for optimizing and evaluating the quantized model, termed Attention Distribution Alignment (ADA). ADA enhances the quantization-aware training process by explicitly aligning salient feature regions between full-precision and quantized models through attention-based feature representations.

In summary, the contributions of this paper are as follows:

- We provide the first in-depth analysis of the root causes

behind performance degradation in low-bit quantization of multi-task neural network models, identifying misaligned feature fusion and biased gradient optimization as critical bottlenecks during quantization-aware training.

- We propose the Gradient-Aware Balanced Feature Fusion (GABFusion) approach, which integrates task-adaptive fusion factors and gradient-balancing normalization to effectively reduce gradient disparity across network branches designed for different tasks.
- We introduce an Attention Distribution Alignment (ADA) strategy that enables feature-level alignment between quantized and full-precision models, providing more accurate informative supervision signals for quantization-aware training.
- Extensive experiments demonstrate that our strategy generalizes well across diverse network architectures and QAT algorithms, achieving superior performance over state-of-the-art QAT approaches. Notably, when applied to YOLOv5 under a 4-bit quantization setting, our approach reduces the accuracy gap with the full-precision baseline to only 1.7% on the VOC dataset.

Related Work

Quantization of Deep Neural Networks

Quantization compresses neural networks by mapping weights and activations to lower precision, reducing storage and computation. Methods include *Post-Training Quantization* (PTQ), which requires no retraining and uses a small calibration set, and *Quantization-Aware Training* (QAT), which inserts fake quantization and applies the *Straight-Through Estimator* (STE)(Bengio, Léonard, and Courville 2013) for gradient approximation, trading higher training cost for better accuracy. Classic PTQ methods such as AdaRound(Nagel et al. 2020), BRECQ(Li et al. 2021), and QDrop(Wei et al. 2022) have demonstrated strong performance under 8-bit quantization. However, at lower bit-widths, QAT methods show significantly superior results. Representative state-of-the-art QAT approaches include: PACT(Choi et al. 2018), which suppresses activation outliers to reduce quantization error; LSQ(Esser et al. 2020), which jointly optimizes weights and scaling factors during training; LSQ+(Bhalgat et al. 2020), which further introduces learnable offsets and improved initialization strategies; and N2UQ(Liu et al. 2022), which learns input thresholds to enhance representational flexibility while maintaining hardware-friendly uniform quantization.

These methods achieve impressive accuracy in low-bit classification tasks and can even outperform full-precision models under low-bit settings. Nonetheless, when applied to multi-task scenarios, they suffer from notable accuracy degradation—highlighting that current methods overlook fundamental issues such as task-specific feature discrepancies and gradient conflicts. To the best of our knowledge, this work is the first to formally identify these problems and propose a unified optimization strategy to address them.

Quantization in Multi-Task Learning

Multi-task learning seeks to optimize multiple tasks concurrently within a single network framework(Jeong and Yoon 2024). Within the domain of computer vision, the YOLO series of object detection models has emerged as a predominant approach, distinguished by its high accuracy and rapid inference capabilities. Recent studies have shown that PTQ scheme can quantize the YOLO model with near full-precision accuracy at 8-bit precision(Wang et al. 2023). However, significant accuracy degradation still persists when low-bit (≤ 4 -bit) configuration are used. To improve the performance of the quantized model, The work of (Huang et al. 2024) refined the loss functions to balance classification and regression tasks and applied them to existing QAT methods. (Gupta and Asthana 2024) introduced weight smoothing and correction techniques to mitigate oscillation caused by quantization noise. While these approaches alleviate performance degradation to some extent, substantial accuracy gaps still remained. Some studies (Ding et al. 2024; Chu, Li, and Zhang 2024) attempt to improve quantized model performance by modifying the network architecture, such as replacing the original CSP backbone of YOLO with more quantization-friendly structures. However, such changes often disrupt the original YOLO design, leading to degraded baseline performance and limited practical applicability.

The goal of this work is to develop a general optimization framework that can be seamlessly integrated with any state-of-the-art QAT method to substantially enhance the performance of quantized models, while requiring no modifications to the original neural network architecture.

Proposed Method

Problem Formulation

During the quantization-aware training process, each layer introduces quantization error. Let x_l denote the full-precision output of the l -th layer, and \tilde{x}_l its quantized counterpart. The quantization error is defined as $\delta_l = \tilde{x}_l - x_l$. Since the input to the l -th layer is also quantized, we have $\tilde{x}_{l-1} = x_{l-1} + \delta_{l-1}$, leading to the perturbed output: $\tilde{x}_l = f_l(\tilde{x}_{l-1}) + \epsilon_l \approx f_l(x_{l-1} + \delta_{l-1}) + \epsilon_l$, where $f_l(\cdot)$ is the transformation of the l -th layer (e.g., convolution and activation), and ϵ_l represents the new quantization noise. Assuming δ_{l-1} is small, a first-order approximation gives: $f_l(x_{l-1} + \delta_{l-1}) \approx f_l(x_{l-1}) + J_l \delta_{l-1}$, where J_l is the Jacobian matrix of f_l with respect to its input. Thus, the total error propagates as:

$$\delta_l \approx J_l \delta_{l-1} + \epsilon_l \quad (1)$$

This shows that errors from shallow layers propagate through Jacobian transformations and accumulate with layer-wise noise ϵ_l , resulting in inevitable error accumulation.

In the multi-task scenario, classification and regression tasks are often both involved. While cross-entropy loss—widely used for classification—has been successfully applied to training quantized neural networks with certified robustness guarantees (Lechner et al. 2023), our focus is on

regression tasks that demand high pixel-level precision, exemplified by the commonly used CIoU loss in object detection (Zheng et al. 2020). To fully leverage shallow and deep feature information, models typically fuse the shallow output \tilde{F}_s and the deep output \tilde{F}_d . For example, fusion can be performed via concatenation: $\tilde{F}_{\text{cat}} = [\tilde{F}_s; \tilde{F}_d]$.

Let the model predict the target center offset as \hat{t} , with the ground truth denoted as t^* . The prediction is formed as a linear combination of \tilde{F}_s and \tilde{F}_d :

$$\hat{t} = \mathbf{w}_s^\top \tilde{F}_s + \mathbf{w}_d^\top \tilde{F}_d = \mathbf{w}_s^\top (F_s + \delta_s) + \mathbf{w}_d^\top (F_d + \delta_d) \quad (2)$$

where \mathbf{w}_s and \mathbf{w}_d represent the linear weights for the shallow and deep features, respectively. F_s and F_d denote the full-precision feature outputs, and δ_s, δ_d represent the corresponding quantization errors.

Since the CIoU loss involves a squared deviation term related to the center prediction error ($\hat{t} - t^*$), it can be simplified as:

$$L_{\text{CIoU}} \propto (\hat{t} - t^*)^2 \quad (3)$$

Expanding the error term yields:

$$\hat{t} - t^* = \mathbf{w}_s^\top \delta_s + \mathbf{w}_d^\top \delta_d + \mathbf{w}_s^\top F_s + \mathbf{w}_d^\top F_d - t^* \quad (4)$$

As in the analysis of Fig. 3, one can examine the gradient flow to identify which features the network prioritizes during training. During the quantization fine-tuning phase, the training initializes from a model that has already fully converged in full-precision, so the gradients mainly originate from $\mathbf{w}_s^\top \delta_s + \mathbf{w}_d^\top \delta_d$. Due to the accumulation of quantization noise across layers, the disturbance term from deep features $\mathbf{w}_d^\top \delta_d$, contributes more to the final error $\hat{t} - t^*$ than the shallow counterpart $\mathbf{w}_s^\top \delta_s$. To minimize the loss, the network amplifies its response to error-dominated features and receives stronger gradient signals from deeper layers during backpropagation, thereby prioritizing updates to the deep features \tilde{F}_d while neglecting essential fine-grained details. This effect can be quantified by the following gradient inequality:

$$\left| \frac{\partial L_{\text{CIoU}}}{\partial \tilde{F}_d} \right| \gg \left| \frac{\partial L_{\text{CIoU}}}{\partial \tilde{F}_s} \right| \quad (5)$$

It also highlights an important insight: relying solely on numerical perturbation-based loss supervision during quantization training is insufficient to reflect the model’s decision-making capacity, as decisions are ultimately made based on feature representations.

Gradient-Aware Balanced Feature Fusion

To tackle the above issue, we propose a Gradient-Aware Balanced Feature Fusion strategy, a simple yet effective solution tailored to the identified gradient bias problem. Its strength lies not in architectural complexity, but in the precise alignment between problem, mechanism, and solution. The algorithmic procedure is summarized in Algorithm 1.

Firstly, we introduce a learnable weight parameter $\alpha \in [0, 1]$ to rescale the shallow feature branch \tilde{F}_s and deep feature branch \tilde{F}_d before fusion:

$$F'_s = \alpha \cdot \tilde{F}_s, \quad F'_d = (1 - \alpha) \cdot \tilde{F}_d \quad (6)$$

The learnable weight α enables adaptive control over the fusion ratio of \tilde{F}_s and \tilde{F}_d . The rescaled features are concatenated along the channel dimension to obtain the fused representation $F'_{\text{cat}} = [F'_s; F'_d]$. For each spatial position (i, j) , let the concatenated vector be $\mathbf{h} = F'_{\text{cat}}(i, j)$ with a length of $C_s + C_d$, where C_s and C_d denote the channel dimensions of the shallow and deep features, respectively.

Secondly, a LayerNorm(?) module is inserted immediately after the feature fusion layer as a one-time plug-in component, which performs normalization across all channels at each spatial location, effectively centralizing and scaling the gradients — akin to gradient whitening. Note that the LayerNorm modules can be safely removed from the original network during inference, as they primarily serve to stabilize feature distributions and gradient flow during training. Once the quantization parameters have been learned, the normalization no longer contributes to model expressiveness or performance at inference time, and can thus be folded or omitted to reduce computational overhead. The mean μ and standard deviation σ are calculated across the feature dimension of each input sample:

$$\mu = \frac{1}{C_s + C_d} \sum_{k=1}^{C_s+C_d} h_k, \quad (7)$$

$$\sigma = \sqrt{\frac{1}{C_s + C_d} \sum_{k=1}^{C_s+C_d} (h_k - \mu)^2} \quad (8)$$

And the features of each dimension are normalized:

$$\text{LN}(h_k) = \frac{h_k - \mu}{\sigma}, \quad k = 1, \dots, C_s + C_d \quad (9)$$

Let L denote the loss function. According to the chain rule (see **Appendix** for detailed derivation), the gradient of the pre-normalized feature h_k is given by:

$$\frac{\partial L}{\partial h_k} = \frac{1}{\sigma} \left(\frac{\partial L}{\partial \text{LN}(h_k)} - \frac{1}{C_s + C_d} \sum_j \frac{\partial L}{\partial \text{LN}(h_j)} \right) \quad (10)$$

It can be observed that the gradient of each dimension is divided by the same σ and subtracted with the same mean. As a result, gradients of the shallow branch are relatively amplified, while those of the deep branch are suppressed. Combined with the effect of the learnable weight α , the proposed approach encourages both branches to contribute equally to the optimization process, promoting balanced representation learning.

Attention Distribution Alignment

As previously noted, conventional quantization methods primarily rely on numerical deviations from ground truth for loss supervision, yet this approach often overlooks the critical role of feature representations in multi-task learning. Since each task depends on distinct features for decision-making, and different features exhibit varying quantization sensitivity and robustness, it is necessary to introduce supervision strategies based on feature importance to guide quantization training.

Algorithm 1 Gradient-Aware Balanced Feature Fusion

Input: Shallow feature \tilde{F}_s , deep feature \tilde{F}_d **Parameter:** Learnable scalar $\alpha \in [0, 1]$ **Output:** Fused feature F_{out}

- 1: Compute $F'_s = \alpha \cdot \tilde{F}_s$ and $F'_d = (1 - \alpha) \cdot \tilde{F}_d$.
 - 2: Fuse the scaled features: $F_{\text{fused}} = \text{Fuse}(F'_s, F'_d)$.
 - 3: **for all** spatial location (b, i, j) **do**
 - 4: Extract $\mathbf{h} = F_{\text{fused}}(b, :, i, j)$.
 - 5: Compute mean $\mu = \text{Mean}(\mathbf{h})$ and std $\sigma = \text{Std}(\mathbf{h})$.
 - 6: Normalize: $F_{\text{fused}}(b, :, i, j) = (\mathbf{h} - \mu)/\sigma$.
 - 7: **end for**
 - 8: **return** $F_{\text{out}} = F_{\text{fused}}$.
-

Early approaches typically used binarized representations as teacher models and applied knowledge distillation to guide network quantization (Zhu, He, and Wu 2023). However, the limited representational capacity of binary models hinders effective semantic transfer. Therefore, it is desirable to adopt a statistical strategy to maximally extract and utilize the information distribution from full-precision features. Inspired by this, we consider leveraging attention mechanisms to model important features. However, conventional attention mechanisms (Woo et al. 2018) require training to learn attention weights, introducing additional parameters. To address this challenge, we introduce a parameter-free attention mechanism that aligns quantized and full-precision features based solely on statistical principles. In this context, SimAM (Simple, Parameter-Free Attention Module) (Yang et al. 2021) emerges as a compelling choice. Building upon this analysis, we adopt a task-aware perspective that emphasizes the modeling of intermediate feature and propose a feature-level distillation strategy, namely Attention Distribution Alignment (ADA), to enhance the robustness and discriminability of quantized models.

Specifically, we first employ SimAM to extract attention distributions from both the quantized and full-precision models. Given a feature map $X \in R^{C \times H \times W}$, SimAM computes attention independently within each channel. For a spatial position (i, j) , let x_{ij} denote the activation at that location, and let μ_x and σ_x^2 represent the mean and variance of the corresponding channel, respectively. SimAM defines an inverse energy score for each position to quantify its distinctiveness relative to other positions in the same channel:

$$E_{ij}^{-1} = \frac{(x_{ij} - \mu_x)^2}{4(\sigma_x^2 + \lambda)} + 0.5 \quad (11)$$

where λ is a small balancing constant. The inverse energy is then passed through a sigmoid function σ to obtain an attention weight between 0 and 1: $A_{ij} = \sigma(E_{ij}^{-1})$. Finally, the original feature x_{ij} is reweighted by A_{ij} to produce the output: $\tilde{x}_{ij} = A_{ij}x_{ij}$. As a result, important features are effectively highlighted. We then adopt a pretrained full-precision model as the teacher and extract its attention distribution A^f as the ideal focus pattern. The corresponding attention distribution A^q is obtained from the quantized model. To enable distribution alignment, A^f and A^q are normalized into probability distributions P and Q , respectively.

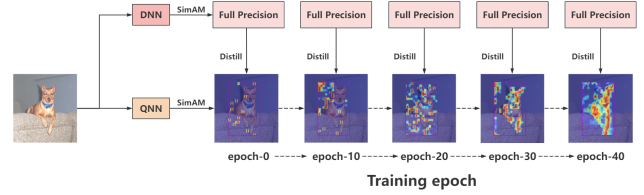


Figure 4: The work flow of ADA. DNN represents the full-precision baseline model, while QNN denotes quantized model. Highlight regions in the heatmap represent attention areas of critical semantic information.

To measure the discrepancy between the two distributions, we take Jensen-Shannon (JS) divergence as an example to construct a feature-level distillation loss L_{JS} that guides the quantized model to learn a more consistent attention pattern. The process is defined as:

$$D_{JS}(P|Q) = \frac{1}{2} \sum_{i,j} P_{ij} \log \frac{P_{ij}}{M_{ij}} + \frac{1}{2} \sum_{i,j} Q_{ij} \log \frac{Q_{ij}}{M_{ij}} \quad (12)$$

where $M = \frac{1}{2}(P + Q)$ denotes the intermediate distribution. During training, this is used as one of the loss terms, i.e., $L_{JS} = D_{JS}(P|Q)$. It is worth noting that the choice of divergence is not unique. We will compare different metrics in the ablation study to evaluate their impact on model performance.

As illustrated in Fig. 4, directly applying the original quantization method during the early stage of training results in a substantial loss of crucial attention information, particularly concerning the perception of target regions. As the distillation progresses, the attention features of the quantized model are gradually recovered, leading to more accurate localization and representation of the target areas.

Experiments

Experimental Setup

The proposed optimization strategy is evaluated on the PASCAL VOC (Everingham et al. 2010) and COCO (Lin et al. 2014) benchmarks. The mean Average Precision (mAP) is used as the evaluation metric. All experiments are conducted on a server equipped with $8 \times$ NVIDIA GeForce RTX 4090 GPUs, each with 24GB of memory. All other training hyper-parameters are kept identical across comparison groups to ensure fair evaluation (see **Appendix** for full details). To verify the generality and effectiveness of the proposed strategy in multi-task scenarios, we integrate it into four representative state-of-the-art low-bit quantization-aware training methods: N2UQ (Liu et al. 2022), PACT (Choi et al. 2018), LSQ (Esser et al. 2020), and LSQ+ (Bhalgat et al. 2020). Taking YOLOv5s and YOLOv11s as the baseline models for multi-task detection.

Experimental Results on the Pascal VOC Dataset

The PASCAL VOC dataset consists of natural images from 20 different categories. We train the models on the combined

training sets of VOC 2007 and VOC 2012, and evaluate their performance on the VOC 2007 test set. The results under two different bit-width configurations, corresponding to 4-bit and 3-bit quantization of weights and activations, respectively—are summarized in Table 1.

Under the W4A4 quantization setting, our method improves the AP_{50} by approximately 2.4% on average across multiple quantization algorithms for both YOLOv5s and YOLOv11s. In the more challenging W3A3 configuration, the performance gain increases to an average improvement of 3.9%. As bit-width decreases, quantization noise becomes increasingly severe and imbalanced across feature branches. The proposed strategy mitigates this issue by balancing feature gradient distributions, thereby achieving greater performance improvements under low-bit settings. Notably, when integrated with the state-of-the-art QAT method N2UQ, the quantized model achieves near-parity with its full-precision counterpart under W4A4, exhibiting only a 1.7% drop in accuracy.

Method	BW	YOLOv11s	YOLOv5s
		AP_{50}	AP_{50}
Full-Precision	FP32	89.4%	85.9%
N2UQ	W4A4	86.2%	82.1%
N2UQ + Ours	W4A4	87.4%	84.2%
PACT	W4A4	83.8%	79.1%
PACT + Ours	W4A4	84.8%	80.6%
LSQ	W4A4	82.9%	76.9%
LSQ + Ours	W4A4	84.2%	78.9%
LSQ+	W4A4	76.8%	67.0%
LSQ+ + Ours	W4A4	80.9%	74.2%
N2UQ	W3A3	83.0%	75.5%
N2UQ + Ours	W3A3	84.3%	78.0%
PACT	W3A3	75.1%	62.9%
PACT + Ours	W3A3	78.2%	66.6%
LSQ	W3A3	75.5%	59.9%
LSQ + Ours	W3A3	78.9%	66.8%
LSQ+	W3A3	73.4%	54.2%
LSQ+ + Ours	W3A3	75.8%	62.5%

Table 1: Demonstration of the generalizability of our strategy across QAT methods (VOC).

Experimental Results on the COCO Dataset

Following the previous section, we further validate the effectiveness of our proposed strategy on the COCO dataset. COCO is a standard open-source benchmark with 80 categories, widely used for evaluating multi-task quantization methods. For clarity, only the best-performing configuration combined with N2UQ is reported in the main paper, with additional results deferred to the **Appendix**. We compare our

Method	BW	YOLOv5s		YOLOv11s	
		AP_{50}	mAP	AP_{50}	mAP
Full-Precision	FP32	56.8%	37.4%	63.9%	47.0%
PACT	W4A4	45.3%	28.3%	51.2%	35.5%
LSQ	W4A4	44.8%	26.9%	49.4%	33.0%
LSQ+	W4A4	44.7%	26.7%	50.0%	34.0%
Q-YOLO	W4A4	26.2%	14.0%	–	–
N2UQ	W4A4	50.2%	31.1%	57.0%	40.2%
N2UQ + EMA	W4A4	51.0%	32.2%	57.6%	40.5%
N2UQ + Ours	W4A4	51.4%	33.2%	58.3%	41.2%
N2UQ + EMA + Ours	W4A4	52.0%	34.0%	58.9%	41.7%

Table 2: Comparison of our strategy with mainstream quantization methods on COCO.

method with representative low-bit quantization approaches that employ the same baseline network. As shown in Table 2, the results for Q-YOLO are taken from (Wang et al. 2023), while all other results are reproduced under our experimental setup, as the original works did not evaluate their methods on the multi-task YOLO architecture used in this study.

As shown in Table 2, our approach consistently outperforms the EMA strategy proposed by (Gupta and Asthana 2024), which is specifically designed for YOLO quantization and has demonstrated strong performance. By reducing gradient oscillations caused by the approximation in the Straight-Through Estimator (STE), EMA significantly enhances the stability of QAT training. However, despite mitigating these oscillations, feature optimization bias remains a challenge in multi-task settings. When our method is further integrated with EMA, an average performance improvement of approximately **1.3%** is achieved, clearly demonstrating the compatibility and composability of our strategy with existing QAT techniques.

Visual and Qualitative Analysis

We visualize the operational mechanism of the proposed strategy during both the forward and backward propagation stages. During the forward pass, multi-scale features from different semantic levels are fused, as illustrated in Fig. 5(a). Our method effectively aligns these features to a unified scale range. In the backward pass, it significantly mitigates the feature gradient imbalance caused by accumulated quantization noise. Specifically, the gradients are rescaled to more uniform magnitudes, as shown in Fig. 5(b), thereby correcting the optimization bias observed in Fig. 3.

Analyzing the Impacts on Regression Tasks

As outlined in previous sections, the primary source of accuracy degradation in multi-task learning stems from the regression branch. To more intuitively illustrate the limitations of conventional quantization methods in regression-based localization tasks, we analyze the distribution of a canonical regression metric—**Intersection over Union (IoU)**—as depicted in Fig. 6(a). It can be observed that, due to imbalanced gradients optimization across feature branches, the baseline

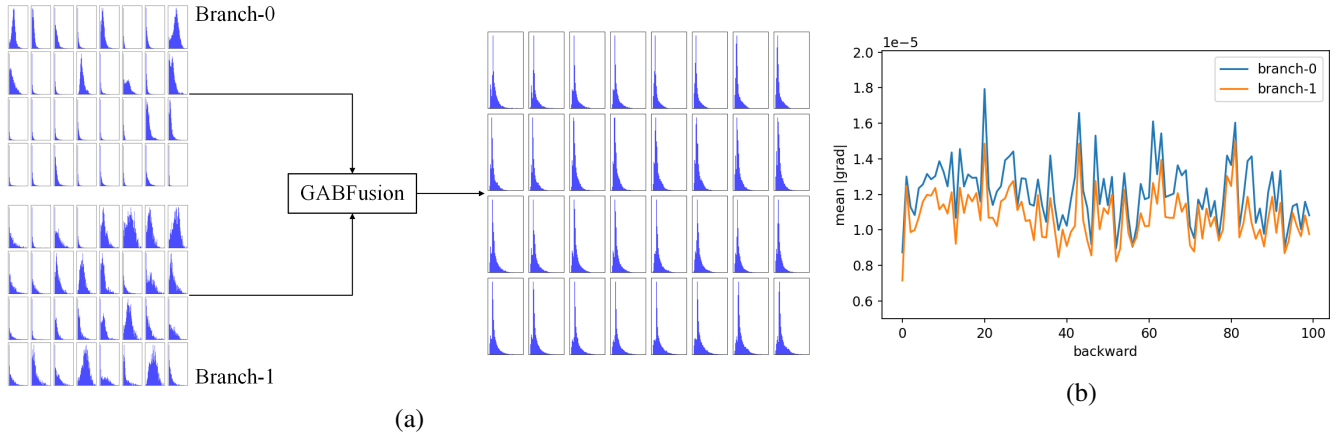


Figure 5: (a) Visualization of the proposed strategy during the feature fusion process. A subset of 32 representative channels is displayed for clarity. (b) Average gradient magnitude at the feature fusion node in YOLOv5 after applying the proposed optimization strategy under quantization.

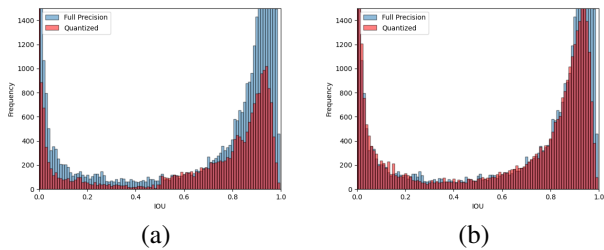


Figure 6: Comparison of the IOU distribution before and after quantization. (a) Result of the baseline quantized model using the original N2UQ method; (b) Result obtained after applying the proposed strategies.

quantized model exhibits a notable drop in high-quality predictions ($\text{IoU} \geq 0.5$), indicating a significant loss of fine-grained information. In contrast, as shown in Fig. 6(b), our proposed method substantially enhances the model’s sensitivity and adaptability to detailed features, thereby recovering a considerable number of high-quality bounding box predictions.

Ablation Study

In this section, we conduct ablation study on the VOC dataset to evaluate the effectiveness of each proposed component. Specifically, GABFusion denotes the proposed Gradient-Aware Balanced strategy, while KL and JS represent two loss evaluation metrics used in the Attention Distribution Alignment strategy, respectively.

As shown in Table 3, the proposed GABFusion strategy consistently delivers stable and significant improvements across all evaluated methods, yielding gains of approximately 1%–5% under both 4-bit and 3-bit quantization settings. When further integrated with the ADA strategy, the quantized models converge to better optima, demonstrating enhanced optimization stability and accuracy. No-

Strategy	N2UQ		LSQ		PACT	
	W4A4	W3A3	W4A4	W3A3	W4A4	W3A3
Baseline	82.1%	75.5%	76.9%	59.9%	79.1%	62.9%
+GABFusion	83.5%	77.4%	78.4%	64.5%	80.2%	65.1%
+GABFusion+KL	83.8%	77.5%	78.9%	66.8%	80.6%	66.6%
+GABFusion+JS	84.2%	78.0%	78.4%	65.8%	80.5%	65.4%

Table 3: Ablation study on the impact of GABFusion and ADA strategies.

tably, quantization methods exhibits varying responses to KL and JS divergences. KL divergence, which is sensitive to low-probability regions, is particularly well-suited for methods like PACT and LSQ that impose bounded activation ranges, enabling finer discrimination of distributional differences within constrained intervals. In contrast, JS divergence is symmetric and more robust to global distribution shifts, making it a preferable choice for methods like N2UQ that incorporate nonlinear transformations. These observations suggest that divergence selection should be aligned with the underlying distribution modeling and representational characteristics of the quantization strategy.

Conclusion

We presented GABFusion, a lightweight and effective fusion strategy for multi-task quantization-aware training. By combining task-adaptive feature fusion with gradient-balancing normalization, it alleviates gradient conflicts and improves task-specific learning. Additionally, the proposed attention distribution alignment loss further enhances quantized model optimization. While our experiments focus on convolution-based multi-task networks like YOLO, future work could explore applying GABFusion to transformer-based unified multi-task architectures, which remain under-explored in low-bit quantization research.

References

- Ba, J. L.; Kiros, J. R.; and Hinton, G. E. 2016. Layer normalization. *arXiv preprint arXiv:1607.06450*.
- Bengio, Y.; Léonard, N.; and Courville, A. 2013. Estimating or propagating gradients through stochastic neurons for conditional computation. *arXiv preprint arXiv:1308.3432*.
- Bhalgat, Y.; Lee, J.; Nagel, M.; Blankevoort, T.; and Kwak, N. 2020. LSQ+: Improving low-bit quantization through learnable offsets and better initialization. In *2020 IEEE/CVF Conference on Computer Vision and Pattern Recognition Workshops (CVPRW)*, 2978–2985.
- Cao, Y.; Xu, J.; Lin, S.; Wei, F.; and Hu, H. 2023. Global Context Networks. *IEEE Transactions on Pattern Analysis and Machine Intelligence*, 45(6): 6881–6895.
- Chen, W.; Xie, D.; Zhang, Y.; and Pu, S. 2019. All You Need Is a Few Shifts: Designing Efficient Convolutional Neural Networks for Image Classification. 7234–7243.
- Choi, J.; Wang, Z.; Venkataramani, S.; Chuang, P.; Srivasan, V.; and Gopalakrishnan, K. 2018. PACT: Parameterized Clipping Activation for Quantized Neural Networks.
- Chu, X.; Li, L.; and Zhang, B. 2024. Make RepVGG Greater Again: A Quantization-Aware Approach. In *Proceedings of the AAAI Conference on Artificial Intelligence*, volume 38, 11624–11632.
- Colbert, I.; Pappalardo, A.; and Petri-Koenig, J. 2023. A2Q: Accumulator-Aware Quantization with Guaranteed Overflow Avoidance. In *2023 IEEE/CVF International Conference on Computer Vision (ICCV)*, 16943–16952.
- Ding, Y.; Feng, W.; Chen, C.; Guo, J.; and Liu, X. 2024. Reg-PTQ: Regression-specialized Post-training Quantization for Fully Quantized Object Detector. In *2024 IEEE/CVF Conference on Computer Vision and Pattern Recognition (CVPR)*, 16174–16184.
- Esser, S. K.; McKinstry, J. L.; Bablani, D.; Appuswamy, R.; and Modha, D. S. 2020. LEARNED STEP SIZE QUANTIZATION. In *International Conference on Learning Representations*.
- Everingham, M.; Gool, L. V.; Williams, C. K. I.; Winn, J.; and Zisserman, A. 2010. The Pascal Visual Object Classes (VOC) Challenge. *International Journal of Computer Vision*, 88(2): 303–338.
- Gupta, K.; and Asthana, A. 2024. Reducing the Side-Effects of Oscillations in Training of Quantized YOLO Networks. In *2024 IEEE/CVF Winter Conference on Applications of Computer Vision (WACV)*, 2440–2449.
- He, K.; Gkioxari, G.; Dollár, P.; and Girshick, R. 2017. Mask R-CNN. In *2017 IEEE International Conference on Computer Vision (ICCV)*, 2980–2988.
- Huang, L.; Dong, Z.; Chen, S.-L.; Zhang, R.; Ti, S.; Chen, F.; and Yin, X.-C. 2024. HQOD: Harmonious Quantization for Object Detection. In *2024 IEEE International Conference on Multimedia and Expo (ICME)*, 1–6.
- Jeong, W.; and Yoon, K.-J. 2024. Quantifying Task Priority for Multi-Task Optimization. In *2024 IEEE/CVF Conference on Computer Vision and Pattern Recognition (CVPR)*, 363–372.
- Jiang, Z.; Gu, J.; Zhu, H.; and Pan, D. Z. 2023. Pre-RMSNorm and Pre-CRMSNorm transformers: equivalent and efficient Pre-LN transformers. In *Proceedings of the 37th International Conference on Neural Information Processing Systems, NIPS '23*. Red Hook, NY, USA: Curran Associates Inc.
- Lechner, M.; Žikelić, u.; Chatterjee, K.; Henzinger, T. A.; and Rus, D. 2023. Quantization-aware interval bound propagation for training certifiably robust quantized neural networks. AAAI'23/IAAI'23/EAAI'23. AAAI Press. ISBN 978-1-57735-880-0.
- Li, R.; Wang, Y.; Liang, F.; Qin, H.; Yan, J.; and Fan, R. 2019. Fully Quantized Network for Object Detection. In *2019 IEEE/CVF Conference on Computer Vision and Pattern Recognition (CVPR)*, 2805–2814.
- Li, Y.; Dong, X.; and Wang, W. 2020. Additive Powers-of-Two Quantization: An Efficient Non-uniform Discretization for Neural Networks. In *International Conference on Learning Representations (ICLR)*.
- Li, Y.; Gong, R.; Tan, X.; Yang, Y.; Hu, P.; Zhang, Q.; Yu, F.; Wang, W.; and Gu, S. 2021. {BRECQ}: Pushing the Limit of Post-Training Quantization by Block Reconstruction. In *International Conference on Learning Representations*.
- Lin, J.; Tang, J.; Tang, H.; Yang, S.; Chen, W.-M.; Wang, W.-C.; Xiao, G.; Dang, X.; Gan, C.; and Han, S. 2024. AWQ: Activation-aware Weight Quantization for On-Device LLM Compression and Acceleration. In Gibbons, P.; Pekhimenko, G.; and Sa, C. D., eds., *Proceedings of Machine Learning and Systems*, volume 6, 87–100.
- Lin, T.-Y.; Maire, M.; Belongie, S.; Hays, J.; Perona, P.; Ramanan, D.; Dollár, P.; and Zitnick, C. L. 2014. Microsoft COCO: Common Objects in Context. In Fleet, D.; Pajdla, T.; Schiele, B.; and Tuytelaars, T., eds., *Computer Vision – ECCV 2014*, 740–755. Cham: Springer International Publishing. ISBN 978-3-319-10602-1.
- Liu, S.; Qi, L.; Qin, H.; Shi, J.; and Jia, J. 2018. Path Aggregation Network for Instance Segmentation. In *2018 IEEE/CVF Conference on Computer Vision and Pattern Recognition*, 8759–8768.
- Liu, Z.; Cheng, K.-T.; Huang, D.; Xing, E.; and Shen, Z. 2022. Nonuniform-to-Uniform Quantization: Towards Accurate Quantization Via Generalized Straight-Through Estimation. In *2022 IEEE/CVF Conference on Computer Vision and Pattern Recognition (CVPR)*.
- Ma, L.; Zhou, Y.; Ma, J.; Yu, G.; and Li, Q. 2024. One-Step Forward and Backtrack: Overcoming Zig-Zagging in Loss-Aware Quantization Training. In *Proceedings of the AAAI Conference on Artificial Intelligence*, volume 38, 14246–14254.
- Nagel, M.; Amjad, R. A.; Van Baalen, M.; Louizos, C.; and Blankevoort, T. 2020. Up or down? adaptive rounding for post-training quantization. In *Proceedings of the 37th International Conference on Machine Learning, ICML'20*. JMLR.org.
- Rokh, B.; Azarpeyvand, A.; and Khanteymooori, A. 2023. A Comprehensive Survey on Model Quantization for Deep

- Neural Networks in Image Classification. *ACM Trans. Intell. Syst. Technol.*, 14(6).
- Selvaraju, R. R.; Cogswell, M.; Das, A.; Vedantam, R.; Parikh, D.; and Batra, D. 2017. Grad-CAM: Visual Explanations from Deep Networks via Gradient-Based Localization. In *2017 IEEE International Conference on Computer Vision (ICCV)*, 618–626.
- Tong, K.; and Wu, Y. 2024. Small object detection using deep feature learning and feature fusion network. *Engineering Applications of Artificial Intelligence*, 132: 107931.
- Varghese, R.; and M., S. 2024. YOLOv8: A Novel Object Detection Algorithm with Enhanced Performance and Robustness. In *2024 International Conference on Advances in Data Engineering and Intelligent Computing Systems (ADICS)*, 1–6.
- Wang, A.; Chen, H.; Liu, L.; Chen, K.; Lin, Z.; Han, J.; and Ding, G. 2024. YOLOv10: Real-Time End-to-End Object Detection. In Globerson, A.; Mackey, L.; Belgrave, D.; Fan, A.; Paquet, U.; Tomczak, J.; and Zhang, C., eds., *Advances in Neural Information Processing Systems*, volume 37, 107984–108011. Curran Associates, Inc.
- Wang, M.; Sun, H.; Shi, J.; Liu, X.; Cao, X.; Zhang, L.; and Zhang, B. 2023. Q-YOLO: Efficient Inference for Real-Time Object Detection. In Lu, H.; Blumenstein, M.; Cho, S.-B.; Liu, C.-L.; Yagi, Y.; and Kamiya, T., eds., *Pattern Recognition*, 307–321. Cham: Springer Nature Switzerland. ISBN 978-3-031-47665-5.
- Wei, X.; Gong, R.; Li, Y.; Liu, X.; and Yu, F. 2022. QDrop: Randomly Dropping Quantization for Extremely Low-bit Post-Training Quantization. In *International Conference on Learning Representations*.
- Woo, S.; Park, J.; Lee, J.-Y.; and Kweon, I. S. 2018. CBAM: Convolutional Block Attention Module. In Ferrari, V.; Hebert, M.; Sminchisescu, C.; and Weiss, Y., eds., *Computer Vision – ECCV 2018*, 3–19. Cham: Springer International Publishing. ISBN 978-3-030-01234-2.
- Xu, J.; Sun, X.; Zhang, Z.; Zhao, G.; and Lin, J. 2019. *Understanding and improving layer normalization*. Red Hook, NY, USA: Curran Associates Inc.
- Yang, L.; Zhang, R.-Y.; Li, L.; and Xie, X. 2021. SimAM: A Simple, Parameter-Free Attention Module for Convolutional Neural Networks. In Meila, M.; and Zhang, T., eds., *Proceedings of the 38th International Conference on Machine Learning*, volume 139 of *Proceedings of Machine Learning Research*, 11863–11874. PMLR.
- Yang, Y.; Lin, C.; Li, Q.; Zhao, Z.; Fan, H.; Zhou, D.; Wang, N.; Liu, T.; and Shen, C. 2024. Quantization Aware Attack: Enhancing Transferable Adversarial Attacks by Model Quantization. *IEEE Transactions on Information Forensics and Security*, 19: 3265–3278.
- Yuan, Z.; Xue, C.; Chen, Y.; Wu, Q.; and Sun, G. 2022. PTQ4ViT: Post-training Quantization for Vision Transformers with Twin Uniform Quantization. In Avidan, S.; Brostow, G.; Cissé, M.; Farinella, G. M.; and Hassner, T., eds., *Computer Vision – ECCV 2022*, 191–207. Cham: Springer Nature Switzerland. ISBN 978-3-031-19775-8.
- Zheng, Z.; Wang, P.; Liu, W.; Li, J.; Ye, R.; and Ren, D. 2020. Distance-IoU Loss: Faster and Better Learning for Bounding Box Regression. In *Proceedings of the AAAI Conference on Artificial Intelligence*, volume 34, 12993–13000.
- Zhu, K.; He, Y.-Y.; and Wu, J. 2023. Quantized Feature Distillation for Network Quantization. *Proceedings of the AAAI Conference on Artificial Intelligence*, 37(9): 11452–11460.